# Surface Creek Crack Growth Analysis for 316- Stainless Steel

NWE NI TUN[1], ZAR CHI THAUNG[2]
[1] *Mechanical Engineering Department, Mandalay Technological University*
[2] *Mechanical Engineering Department, Technological University (Maubin)*

***Abstract-*** ***The surface creep crack growth analysis is a critical consideration in prediction of remaining life for high temperature structural components. In this research, the remaining life assessment for internal and external surface cracks in a pressurized vessel was conducted by analytical method. The elliptical surface creek crack growth was investigated with various initial aspect ratios in 316- stainless steel. Estimating $C_t$ at both the deepest point and surface point, the aspect ratios of the surface cracks were updated for every time step. Changes of crack depth, crack size, $C^*$ and $C_t$ values at the deepest point and surface point of the crack tip were estimated and used to predict the evolution of crack shape during surface crack growth. It was observed that the remaining life of internal circumferential surface crack was about 53 times longer than that of external axial surface crack at the same crack size and loading conditions. It was also noted that the effects of remaining life, crack propagations and variations of $C_t$ parameters were significantly sensitive to the crack locations and crack depth. There was no obvious convergence of crack aspect ratio observed when crack depth ratio was increased. This method can be extended to various locations of surface crack geometries and various kinds of material properties.***

***Indexed Terms-*** ***Remaining Life Assessments; Pressurized Vessel; Surface Cracks; Creep Crack Growth.***

## I. INTRODUCTION

Remaining life prediction methodology based on time dependent fracture mechanics has been developed and applied successfully in many structural components of power generating industry and process industry such as steam pipes, super-heater headers, turbine rotors, casings and pressure vessels when they have cracks and are operated at elevated temperature [1-6]. In the pressure vessels under operating at high temperatures, the various kinds of failures have been traced to fatigue, creep, stress corrosion and surface crack problem. In case of pressure vessels, the cracks are usually formed at one surface and grow to the other. The presence of surface cracks can significantly reduce the life of structural components. As a result, the remaining life prediction methodology based on time dependent fracture mechanics parameters is required in order to predict the crack growth in a pressurized vessel.

In the time dependent surface crack growth rate for the cases with various material properties, creep condition and surface crack geometries, $C^*$ and $C_t$ are widely used as the fracture parameters [1, 2, 3]. They are equally applicable under the extensive steady state creep stage, but $C^*$ has limitation for application under the small scale creep stage and the transition creep stage. Therefore, $C_t$ is chosen to predict the time dependent crack growth behavior from the small scale creep stage to the extensive steady state creep stage. Little research has been done on estimation of $C_t$ parameter for creep crack growth analysis of external axial and internal circumferential surface cracks in a vessel under various loading conditions. Therefore, the remaining life assessment based on $C_t$ parameter under small scale to extensive creep stage for various crack locations in a pressurized vessel should be extended to the fore-mentioned cases. In this study, remaining life assessment methodology was extended to external axial and internal circumferential surface crack in a pressurize vessel using an analytical method.

## II. GEOMETRICAL DESCRIPTIONS OF THE MODELS

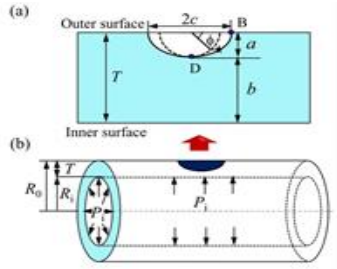


Figure1. Geometry model of external axial surface crack: (a) the sketch of a semi-elliptical axial surface crack; (b) a vessel containing a semi-elliptical surface crack located on the external surface subjected to uniform internal pressure.

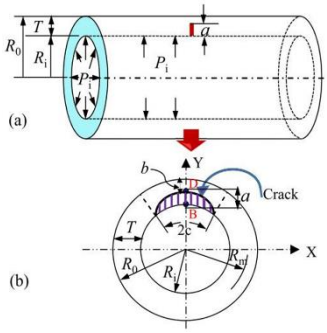


Figure2. Geometry model of internal radial-circumferential surface crack: (a) a vessel containing a semi-elliptical surface crack located on the internal surface subjected to uniform internal pressure; (b) the sketch of a semi-elliptical circumferential surface crack.

A semi-elliptical surface crack of the pressure vessel located in the axial plane on the external surface shown in Fig. 1 was considered. Another case with a surface crack in the radial- circumferential plane on the internal surface shown in Fig.2 was also considered. In both cases, uniform internal pressure loading was assumed. In these figures, the deepest point along the crack front was denoted as location D and the crack tip location on the surface was denoted as location B. Ri, and R0 represent inner and outer radii, respectively, Rm is the mean radius, T is the thickness of the vessel, Pi is the internal pressure, a is the crack depth, b is the size of the un-cracked ligament, c is half of the crack length on the surface, and ϕ is the angular parameter defining the crack front position.

## III. ESTIMATION EQUATIONS FOR SURFACE CRACKED VESSEL

The empirical equations of stress intensity factor, K, for external axial surface crack was derived by Newman and Raju [4]. The ratio of the crack depth to half the crack length on the surface is represented as the aspect ratio, a/c. The crack depth ratio (a/T) can be represented as the ratio of crack depth to wall thickness of the vessel. And the ratio of wall thickness to radius of the vessel is defined as T/R respectively. The K equation within the range of and for external axial surface cracked vessel under tension loading condition is written as [4]:

$$K = \sigma\sqrt{\pi\frac{a}{Q}}F_e\left(\frac{a}{T},\frac{a}{c},\frac{T}{R_i},\phi\right) \quad (1)$$

$$F_e = 0.97\left(m_1 + m_2\left(\frac{a}{T}\right)^2 + m_3\left(\frac{a}{T}\right)^4\right) f_\varphi g f_c\, f_e \quad (2)$$

$$f_c = \left[\frac{\left(1+k^2\right)}{\left(1-k^2\right)} + 1 - 0.5\sqrt{\nu}\right]\left[\frac{T}{R_i}\right] \quad (3)$$

$$f_\phi = \left[\left(\frac{a}{c}\cos\phi\right)^2 + \sin^2\phi\right]^{1/4} \quad (4)$$

$$g = 1 + \left[0.1 + 0.35\left(\frac{a}{T}\right)^2\right]\left(1-\sin\phi\right)^2 \quad (5)$$

$$Q = 1 + 1.464\left(\frac{a}{c}\right)^{1.65} \quad (6)$$

$$f_e = 1.1 \quad (7)$$

Where remote tension is stress and is the boundary correction factor for external axial surface crack and is the shape factor for an elliptical crack. For extending the application to the case of external axial cracked vessel, the remote tension stress, in the equation (1) is replaced by the average hoop stress [5] that has been validated for internal axial surface crack case. The average hoop stress [5] was written as follows:

$$\sigma_h = \frac{P_i R_i}{T} \quad (8)$$

Stress intensity factor equation for internal circumferential surface cracked vessel within the range of, and was developed by Zahoor [6] as follows:

$$K = \sigma_t \sqrt{\pi T} F_c \quad (9)$$

$$F_c = 0.25 + 0.4868\psi + 0.3835\psi^2 + 0.0086\psi\left(\frac{R_m}{T} - 5\right) \quad (10)$$

Where, is the axial tension stress and is the boundary-correction factor for internal circumferential surface crack. The C*-integral equation for the deepest point of an external axial surface crack can be obtained by Eq. (11) as follows:

$$C^* = A.a.(1-\frac{a}{T})h_1(\frac{T}{R_i},\frac{a}{T},n)\left[\frac{\sqrt{3}}{2}\frac{P_i R_i/T}{1-a/T}\right]^{n+1} \quad (11)$$

The C*-integral equation for internal surface crack can be obtained by Eq. (12) as follows:

$$C^* = A.a(1-\frac{a}{T})h_1(\frac{T}{R_i},\frac{a}{T},n)\left[\frac{\sqrt{3}\sigma}{2(1-a/T)}\right]^{n+1} \quad (12)$$

In order to characterize the crack growth rate from small-scale to extensive steady-state creep conditions, a parameter of Ct for elastic-plastic-secondary creeping material is as follows [12]:

$$C_t = \frac{4\alpha\beta\tilde{r}_c(\theta,n)}{E(n-1)}\frac{(1-\nu^2)K^4}{T}\frac{F'}{F}(EA)^{\frac{2}{n-1}}(t+t_{pl})^{-\left[\frac{(n-3)}{(n-1)}\right]} + C^* \quad (13)$$

Where is a scaling factor, E is the Young's modulus, is the Poisson's ratio, K is the stress intensity factor and θ is the angle measured from the crack plane ahead of the crack tip. And t is the elapsed time after loading, is the time for crack tip creep zone development retardation due to crack tip plastic zone and is a dimensionless function of n. Is 1/3 determined by finite dimensionless function dependent on n and θ. At θ = 90˚, a non-dimensional constant for plane strain condition varies approximately from element calculations [3] and is a 0.2 to 0.5 when n varies from 3 to 13. And are K- calibration function and derivative of with respect to in this analysis.

The creep crack growth rate under small scale to transient creep conditions can be characterized by the Eqs. (14) and (15):

$$\frac{da}{dt} = H(C_t)^q \quad (14)$$

$$\frac{dc}{dt} = H(C_t)^q \quad (15)$$

Where, da/dt and dc/dt are the creep crack growth rate along crack depth direction and surface crack length direction, H is creep crack growth coefficient and q is creep crack growth exponent. The critical crack size, was defined as follows in Ref. [15]:

$$a_c = \frac{1}{\pi}\left[\frac{K_{IC}}{1.12\sigma_y}\right]^2 \quad (16)$$

Where, is the critical crack size, is the fracture toughness and is the yield strength.

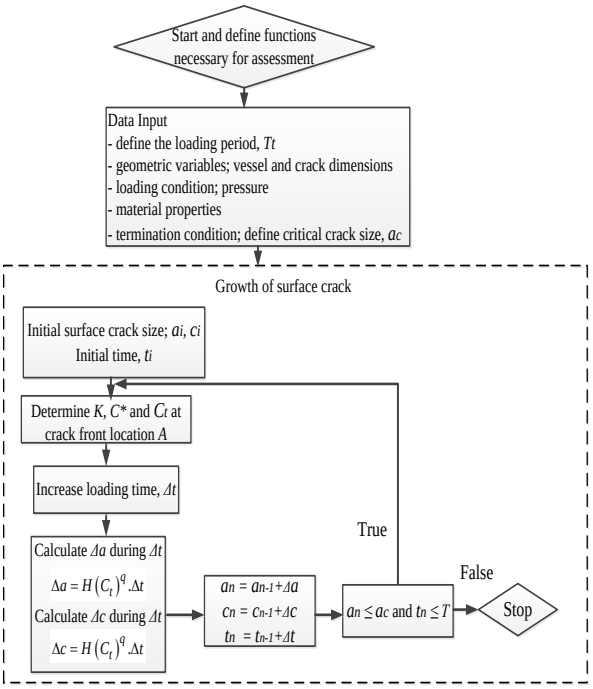


Fig 3. Simulation algorithm for creep crack growth analysis of surface cracked cylinder.

The remaining life assessment for creep crack growth analyses was conducted by developing the conventional code in MATLAB software (R2010b), a structured program, based on the procedure of the algorithm as shown in Fig. 3. In this study, the analysis was terminated when the crack depth exceeds 70% of the thickness or the $a_n > a_c$ condition is satisfied by applying the equation (16). To predict the influence of various initial aspect ratios on crack propagation, two sets of analysis for each crack locations as shown in Figs. 4 and 5 were carried out for the initial crack geometries. To do so, sixteen models with various initial aspect ratios were conducted for completing of two crack cases as shown in Table 2-3. By using the $C_t$ values, changes of aspect ratio, crack depth, crack length and $C_t$ values are estimated with various initial aspect ratios to predict the crack growth.

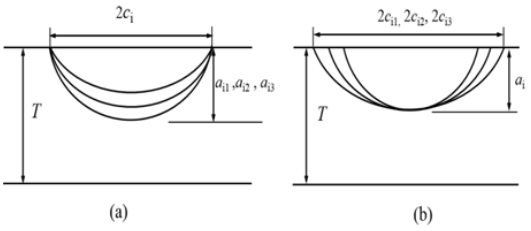


Fig 4. Two sets of initial crack geometries for external radial-axial surface crack: (a) when the initial surface half crack length is fixed; (b) when the initial crack depth is fixed.


Fig 5. Two sets of initial crack geometries for internal radial-circumferential surface crack (a) when the initial circumference half crack length is fixed; (b) when the initial crack is fixed.

Table 1. Material properties of 316-stainless steel

| | |
|---|---|
| Young's Modulus | 193 |
| Poisson's ratio | 0.3 |
| A($MPa^{-n}h^{-1}$) | 1.04 $e^{-22}$ |
| n | 8.2 |
| H | 0.221 |
| q | 0.891 |
| Internal Pressure (MPa) | 9 |

Table 2. Initial aspect ratios when initial crack depth is varied for surface cracks

| | | | | | | |
|---|---|---|---|---|---|---|
| Set $c_i$ = 30.5 mm | $a_i$ (mm) | 17.2 | 18.3 | 19.8 | 21.35 | 24.4 |
| | $a/T$ | 0.45 | 0.48 | 0.52 | 0.56 | 0.64 |
| | $a/c$ | 0.55 | 0.6 | 0.65 | 0.7 | 0.8 |

Table 3. Initial aspect ratios when initial crack depth is fixed for surface cracks

| | | | | | | |
|---|---|---|---|---|---|---|
| Set $a_i$ = 15 mm | $c_i$ (mm) | 30 | 25 | 21.4 | 18.8 | 16.7 |
| | $a/T$ | 0.4 | 0.4 | 0.4 | 0.4 | 0.4 |
| | $a/c$ | 0.5 | 0.6 | 0.7 | 0.8 | 0.9 |

## IV. RESULTS AND DISCUSSIONS

The sensitivity of crack depth and surface crack length growth behaviors as a function of time was depicted in Fig. 6. These were generated by increasing the initial crack depth, ai, and fixing the initial crack length, ci. For the external axial crack, the initial crack depth was varied as as shown in Fig. 6 (a) and the initial crack depth was varied at the internal circumferential crack as shown in Fig.6 (b) respectively. Both the crack depth, a, and crack length, c, increased steadily with time at the external axial crack during the initial

portion of the life. In the internal circumferential crack case, both of crack depth and crack length changed slightly during the initial stage. In both crack cases, the sensitivity increased when the crack depths were closer to the thickness of the cylinder and this phenomenon were also observed in the literature [3]. All the trend of crack depth propagation between initial crack depths variations were ended at the critical crack size. In the crack depth propagation, when the crack depth becomes equal to or greater than a critical value, the crack is expected to become break through the vessel wall. It was observed that the external axial crack was excessively conservative compared with the internal circumferential crack at the same loading and crack size conditions as shown in Fig. 7. The difference of conservatism between two crack locations was found about 0.4% when the aspect ratio was fixed as shown in Fig. 7 (a). When the aspect ratio was smaller, the higher difference of conservatism about 2% was observed in Fig. 7 (b).

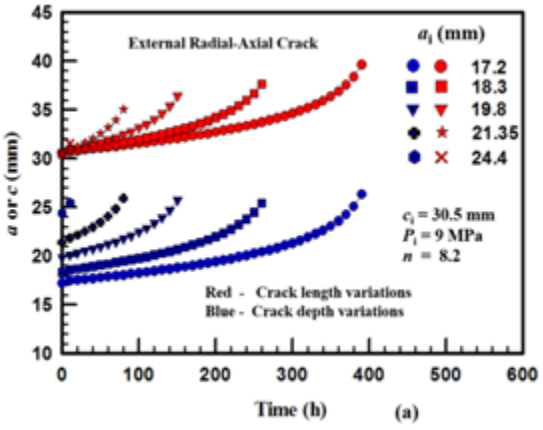


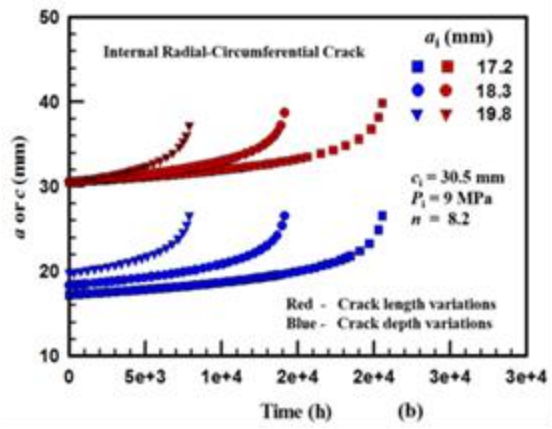


Fig 6. Comparison of crack growth behaviors predicted using different initial crack depths: (a) for external radial-axial crack; (b) for internal radial-circumferential crack.

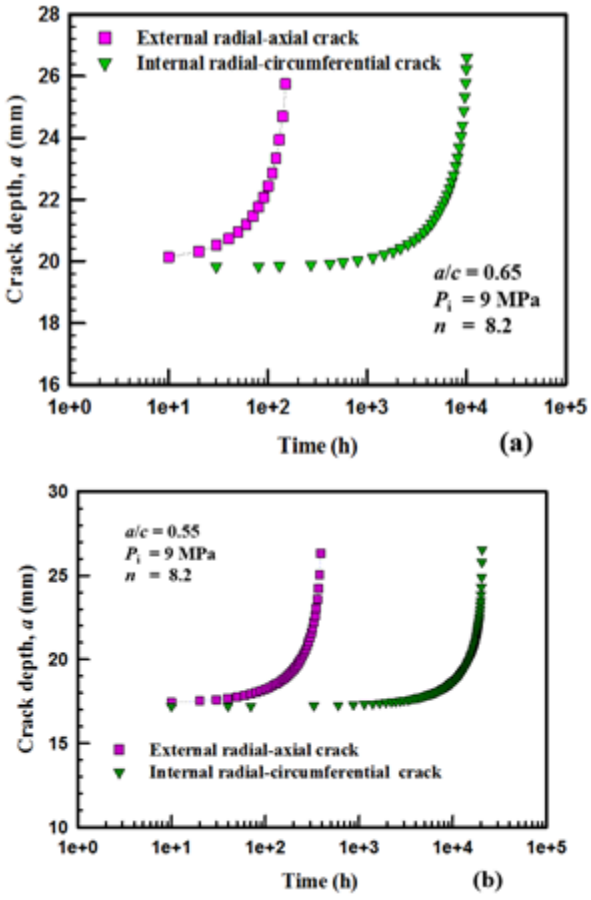


Fig 7. Comparison of crack growth behaviors between two different locations.

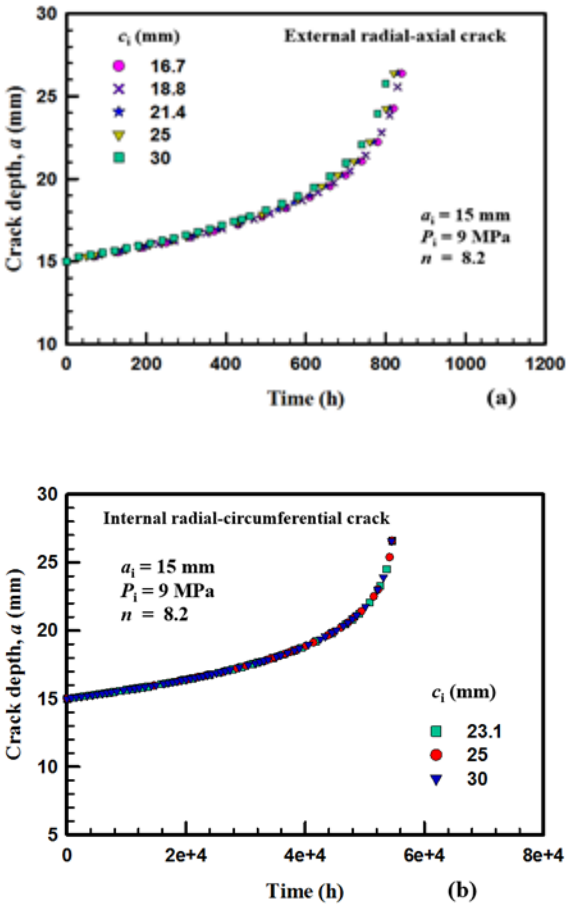


Fig 8. Comparison of crack depth growth behaviors predicted using different initial crack lengths: (a) for external radial-axial crack; (b) for internal radial-circumferential crack.

On the contrary to the first set of analysis, the comparison of crack depth variations predicted using different initial crack lengths and fixing initial crack depth are shown in Fig. 8 for both cracks. The external radial-axial crack growth was predicted when the initial crack length was varied in Fig. 8 (a) and internal radial-circumferential crack growth was predicted when the initial crack length was varied in Fig. 8 (b), respectively. Fig. 8 (a) shows the difference of crack depth variations between the larger initial crack lengths variations cannot be neglected in the external radial-axial crack case. In the internal radial-circumferential crack case, no difference of crack depth variations was observed on the trend, which presented all the crack trends were coincided between the initial crack length variations regardless of the initial aspect ratios as shown in Fig. 8 (b). It can be argued that the crack propagations during crack depth variations are much faster than the propagations during crack length variations in two crack cases.

The comparisons of residual life assessment between two different crack locations were conducted as shown in Fig. 9. Fig. 9 (a) predicted the remaining crack growth life against initial crack depth, ai, when the initial half crack length ci is fixed. It was seen that the remaining life were dependent on the initial crack depth when it was varied. In another set of analysis, the remaining life as a function of the initial half crack length was depicted in Fig. 9 (b). By comparing these two cases, it was shown that the remaining life of internal radial-circumferential crack was about 53 times longer than that of external radial-axial crack at the same crack sizes and loading conditions.

Figure 10 represented the effects of crack aspect ratio (a/c) with increasing crack depth ratio (a/T = 0.45 to 0.64) for two crack locations. The graphs indicated that the trend of aspect ratio in internal radial-circumferential crack were steeper than the trend in external radial-axial crack during the life and that revealed a general trend of considerable increase with increasing a/T.

It was noted that effects of aspect ratio were sensitive to the crack depth ratio a/T. In both cases, no obvious convergence of crack aspect ratio could be observed whatever the crack shape would be. The variations of $C_t$-values during the crack growth life period are illustrated in Fig. 11. For the external crack in Fig. 11 (a), the transition time appears to be approximately a few hours while it appeared within several hours in an internal radial-circumferential crack as indicated in Fig. 11 (b). In both cases, the $C_t$-values approached the $C^*$ values after the transition time. During the last stage of life, the $C_t$-values were increased because the

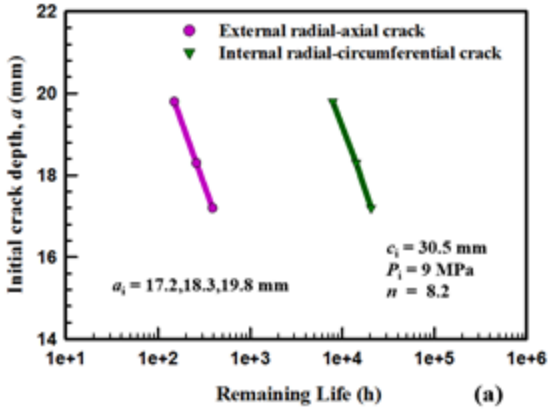


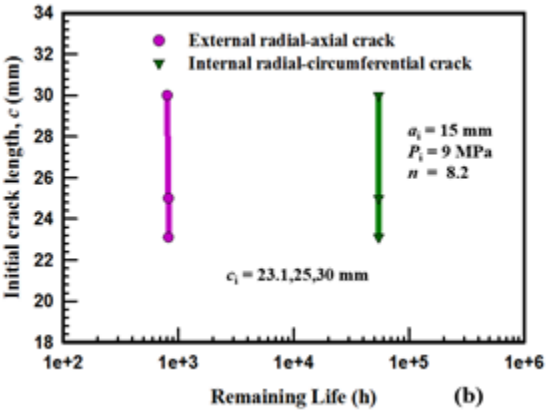


Fig 9. Comparison of Residual life diagrams between two different crack locations: (a) when initial crack depth is varied; (b) when initial crack depth is fixed crack depths increased substantially. In the comparison of Ct-values between two crack locations in Fig. 11 (c), the values of external radial-axial crack were larger than that of internal radial-circumferential crack because of the higher stress influence.

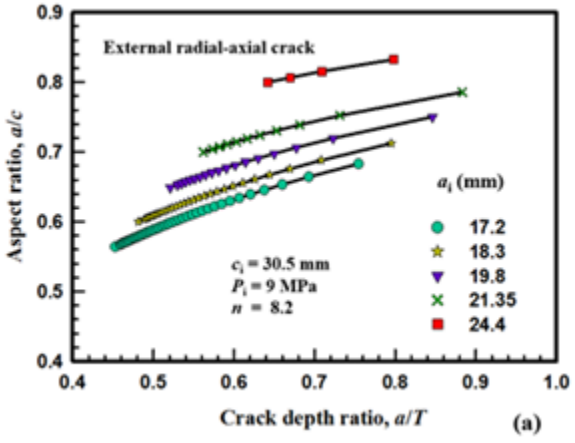


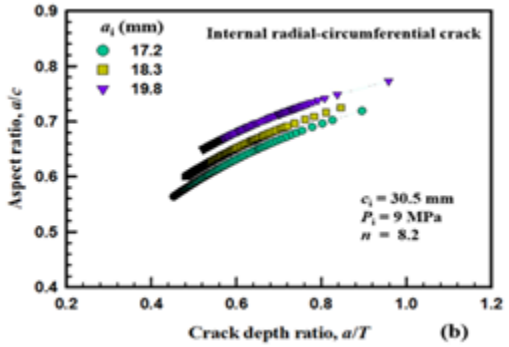


Fig 10. Effect of aspect ratios with increasing crack depth ratios: (a) for external radial-axial crack; (b) for internal radial-circumferential crack.

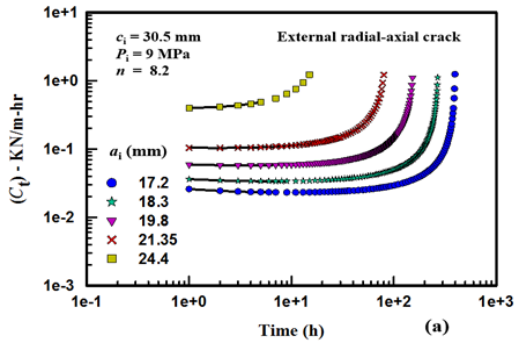


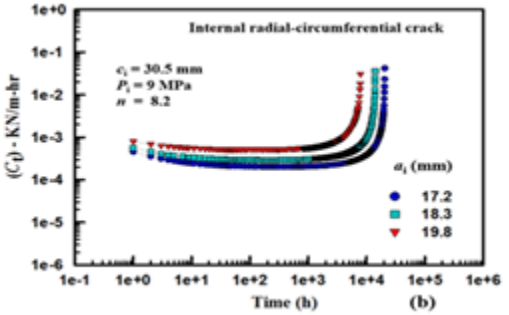

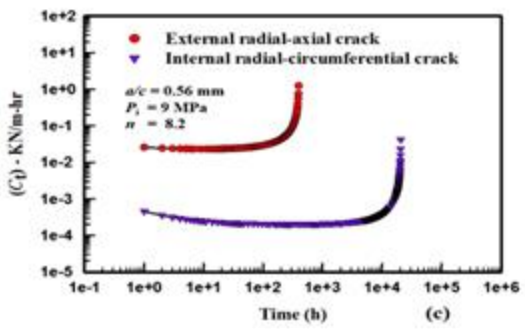


Fig 11. Variations of $C_t$ parameter versus time: (a) for external radial-axial crack; (b) for internal radial-circumferential crack; (c) comparison between two crack locations

## V. CONCLUSION

The prediction of creep crack growth life assessment methodology based on $C_t$ parameter was developed for the case of external radial-axial surface crack and internal radial-circumferential surface crack in a pressurized cylinder. A procedure was extended for estimating K values under the internal pressure loading instead of tension load. The $C^*$ equations were also derived from the fully plastic part of J-integral expressions for surface cracked cylinder subjected to internal pressure.

## ACKNOWLEDGMENT

The first author wishes to acknowledge her deepest gratitude to her parents, professors, relatives and friends to carry out this paper.

## REFERENCES

[1] Wen JF, Tu ST, Gong JM, Sun W. Creep fracture mechanic parameters for internal axial surface cracks in pressurized cylinder and creep growth analysis. Int. J. Pressures Vessel Piping 2011; 88: 452-464.

[2] Kumar Y, Venugopal S, Sasikala G, Albert SK, Bhaduri AK. Study of creep crack growth in a modified 9Cr-1Mo steel weld metal and heat affected zone. Materials Science & Engineering 2016; 655: 300-309.

[3] Yoon KB, Park TG, Saxena A. Creep crack growth analysis of elliptic surface cracks in pressure vessels. International Journal of Pressure Vessels and Piping 2003; 80: 465-79.

[4] Gallagher, Patrick J. USAF damage tolerant design handbook: Guidelines for the Analysis and Design of Damage Tolerant Aircraft Structures, No. FINAL REPO; 1984.

[5] Raju IS, Newman JC. Stress intensity factors for internal and external surface cracks in cylindrical vessels. Journal of Pressure Vessel Technology 1982; 104: 293-298.

[6] Zahoor A. Research project 1757-69. Ductile fracture handbook, vol. 2. Electric Power Research Institute; 1990.

[7] Gortemaker PCM. Application of EPRI handbook to HSST vessel V-1 and comparison with finite element analysis. ECF-6, Amsterdam; 1986.

[8] Kumar V, German MD, Wikening WW. Advances in elastic-plastic fracture analysis. Rep. EPRI, Electric Power Research Institute; 1984.

[9] Saxena A, Yoon KB. Creep crack growth: Assessment of defects in high temperature components. Welding Research Council Bulletin 483; 2003.

[10] Kumar V, German MD, Shih DF. An engineering approach for elastic-plastic fracture analysis. Palo Alto, CA: Electric Power Research Institute; 1981. EPRI-NP-1931, Project 1237-1, Topical Report.

[11] API 579 Second edition. Fitness for service. ASME FFS-1; 2007.

[12] Yoon KB, Saxena A, McDowell DL. Influence of crack-tip cyclic plasticity on creep fatigue crack growth. ASTM STP 1992; 1131: 267-392.

[13] Hormozi R, Biglari F, Nikbin K. Experimental and numerical creep-fatigue study of type 316 stainless steel failure under high temperature LCF loading condition with different hold time. Engineering Fracture Mechanics 2015; 141: 19-43.

[14] Dean DW, Gladwin DN. Creep crack growth behavior of type 316H stainless steels and proposed modifications to standard testing and analysis methods. International Journal of Pressure Vessels and Piping 2007; 84: 378-395.

[15] Saxena A. Nonlinear fracture mechanics for engineers. Boca Raton: CRC press; 1998.